Cell. Mol. Biol. (ISSN: 1165-158X)

Journal Homepage: www.cellmolbiol.org

Cellular and Molecular Biology

Original Article

Green synthesis and characterization of silver nanoparticles from *Ducrosia flabellifolia* Boiss. aqueous extract: Anti-quorum sensing screening and antimicrobial activities against ESKAPE pathogens

Mejdi Snoussi[1,2,3*], Ramzi Hadj Lajimi[4,5], Salman Latif[4], Walid Sabri Hamadou[1], Mousa Alreshidi[1], Syed Amir Ashraf[6], Mitesh Patel[7], Jamal R. Humaidi[4], El Hassane Anouar[8], Adel Kadri[9], Emira Noumi[1,2*]

[1]*Department of Biology, College of Science, Hail University, P.O. Box 2440, Ha'il 2440, Saudi Arabia*
[2]*Laboratory of Genetics, Biodiversity and Valorization of Bio-Resources (LR11ES41), Higher Institute of Biotechnology of Monastir, University of Monastir, Avenue Tahar Haddad, BP74, Monastir 5000, Tunisia*
[3]*Medical and Diagnostic Research Center, University of Ha'il, Hail 55473, Saudi Arabia*
[4]*Chemistry Department, Faculty of Science, Ha'il University, 81451 Hail, P.O. Box 2440, KSA*
[5]*Laboratory of Water, Membranes and Environmental Biotechnologies, Center of Research and Water Technologies, P. B 273, Soliman 8020, Tunisia*
[6]*Department of Clinical Nutrition, College of Applied Medical Sciences, University of Hail, Hail PO Box 2440, Saudi Arabia*
[7]*Research and Development Cell, Department of Biotechnology, Parul Institute of Applied Sciences, Parul University, Vadodara, 391760, India*
[8]*Department of Chemistry, College of Science and Humanities in Al-Kharj, Prince Sattam bin Abdulaziz University, Al-Kharj, Saudi Arabia*
[9]*Faculty of Science and Arts in Baljurashi, Al-Baha University, P.O. Box 1988, Al-Baha 65527, Saudi Arabia*

Article Info

Article history:

Received: September 15, 2023
Accepted: December 02, 2023
Published: February 29, 2024

Use your device to scan and read the article online

Abstract

Biosynthesis of silver nanoparticles using natural compounds derived from plant kingdom is currently used as safe and low-cost technique for nanoparticles synthesis with important abilities to inhibit multidrug resistant microorganisms (MDR). ESKAPE pathogens, especially MDR ones, are widely spread in hospital and intensive care units. In the present study, AgNPs using *Ducrosia flabellifolia* aqueous extract were synthesized using a reduction method. The green synthesized *D. flabellifolia*-AgNPs were characterized by UV–Vis spectrophotometer, Scanning electron microscopy (SEM), and X-ray diffraction assays. The tested *D. flabellifolia* aqueous extract was tested for its chemical composition using Liquid Chromatography-Electrospray Ionization-Mass Spectrometry (LC-ESI-MS). Anti-quorum sensing and anti-ESKAPE potential of *D. flabellifolia*-AgNPs was also performed. Results from LC-ESI-MS technique revealed the identification of chlorogenic acid, protocatechuic acid, ferulic acid, caffeic acid, 2,5-dihydroxybenzoic acid, and gallic acid as main phytoconstituents. Indeed, the characterization of newly synthetized *D. flabellifolia*-AgNPs revealed spherical shape with mean particle size about 16.961±2.914 nm. Bio-reduction of silver was confirmed by the maximum surface plasmon resonance of *D. flabellifolia*-AgNPs at 430 nm. Newly synthetized *D. flabellifolia*-AgNPs were found to possess important anti-ESKAPE activity with low minimal inhibitory concentrations (MICs) ranging from 0.078 to 0.312 mg/mL, and low minimal bactericidal concentrations (MBCs) varying from 0.312 to 0.625 mg/mL. Moreover, *D. flabellifolia*-AgNPs were active against *Candida* utilis ATCC 9255, *C. tropicalis* ATCC 1362, and *C. albicans* ATCC 20402 with high mean diameter of growth inhibition at 5 mg/mL, low MICs, and minimal fungicidal concentrations values (MFCs). The newly synthetized *D. flabellifolia*-AgNPs were able to inhibit violacein production in Chromobacterium violaceum, pyocyanin in *Pseudomonas aeruginosa* starter strains. Hence, the newly synthesized silver nanoparticles using *D. flabellifolia* aqueous extract can be used as an effective alternative to combat ESKAPE microorganisms. These silver nanoparticles can attenuate virulence of Gram-negative bacteria by interfering with the quorum sensing system and inhibiting cell-to-cell communication.

Keywords: *Ducrosia flabellifolia* Boiss.; Silver nanoparticles; Chemical composition; Anti-ESKAPE; Quorum sensing.

1. Introduction

Infectious diseases continue to be an increasing factor of illness and mortality worldwide, reinforced by high resistance of bacterial, mainly bacterial, and viral infections to drugs [1-3]. In addition, the misuse of antibiotics facilitates the development of multidrug-resistant organisms, as well as the appearance of new pathogens against which there is still no treatment [4, 5]. Nowadays, nanomedicine is a rapidly developing field that contributes to the production of a wide range of various synthesized metal

* Corresponding author.
E-mail address: m.snoussi@uoh.edu.sa (M. Snoussi).
Doi: http://dx.doi.org/10.14715/cmb/2024.70.2.13

nanoparticles (MNPs) that explore the possibilities of their uses for the prevention, treatment, diagnosis, and control of disease [6-8]. Additionally, MNPs provide solutions to environmental challenges and are able to surmount some essential problems of conventional small molecules or biomacromolecules (e.g., DNA, RNA, and proteins) and play a dynamic role in introducing various approaches for combating disease, increasing disease diagnostics, and developing new measures for manipulation of plants and pathogens [9].

For instance, application of MNPs has gained tremendous attention due to their specific physiochemical properties such as size, distribution, and morphology, increased electrical conductivity, roughness and the ability to strengthen metals and alloys [10-12]. They have been also studied for their catalytic activity, magnetic, optical, and electronic properties, and antibacterial activity, as well as they are used as assembling of innovative functional materials in medicine, engineering, environment, and agriculture [13-15]. Amongst them, silver nanoparticles (AgNPs) with a diameter of less than 100 nm have gained boundless interest and remain the most noble metal in fabrication of nanoparticles, especially in the field of health and medicine [16]. They are extremely important due to their attractive properties and wide spectrum of anti-inflammatory effects, curing wound healing, microbial proliferation, bactericidal and fungicidal activities as well as their ability to be used in biomedical device coatings, drug-delivery carriers, imaging probes, and diagnostic and optoelectronic platforms [17, 18]. It has been reported that silver nanoparticles possess stronger antibacterial capabilities and are used as anticancer agents [19, 20]. Siver is routinely used in the form of silver nitrate (NO_3^-) for antimicrobial activity. In fact, several multidrug-resistant microorganisms (MDR) circulating in clinical and hospital environments are responsible for several main infections and human diseases (Van Melderen and DeBast, 2009). The emergence of these MDR pathogens can be explicated by the overuse of antibiotics in healthcare, animal, and agriculture sectors [21, 22]. These MDR bacteria are known as ESKAPE pathogens and include *Enterococcus faecium*, *Staphylococcus aureus*, *Klebsiella pneumoniae*, *Acinetobacter baumannii*, *Pseudomonas aeruginosa*, and *Enterobacter* spp. [23-25]. These microorganisms are known to produce exopolysaccharides and are able to adhere to several biotic and abiotic surfaces [26].

Plant-mediated synthesis of nanomaterials known for its eco-friendly nature and cost-effectiveness, aims at decreasing the usage of toxic chemicals, providing a better platform for nanoparticles synthesis since they are safe and contain reducing and capping agents [27, 28]. Extract Ag nanoparticles are important to investigate mainly because they can be used in nanomedicine and are easily packaged in the form of infusions/fluids [16]. This has fascinated scientists to study the way metal ions uptake and bio-reduction by plants. Among various plants, we have chosen *Ducrosia flabellifolia* from Hail region aerial parts extracts for the present study since they have been proven for their potent pharmacological effect [29]. Hence, we newly synthesized silver nanoparticles using *D. flabellifolia* aqueous extract. The chemical composition of the obtained aqueous extract was performed using LC-ESI-MS/MS technique. The characterized silver nanoparticles were tested for their abilities to inhibit the growth of ESKAPE pathogens and Candida species. Moreover, the anti-quorum sensing activities were tested using three starter strains (*Chromobacterium violaceum*, *Pseudomonas aeruginosa*, and *Serratia marcescens*).

2. Material and Methods

2.1. Plant material sampling

Aerial parts from *D. flabellifolia* [30, 31] were collected from the Hail region (Saudi Arabia) in October 2019. For the experiment, 100 g of fresh aerial parts from *D. flabellifolia* plant species (Fig. 1) were grounded and mixed in distilled water (10g plant material+ 100 ml of distilled water), then filtered using Whatman N°1. The filtrate was kept in a dark glass bottle at -4°C till use.

2.2. Phytochemical analysis

The previously validated method was used for the analysis of phenolic compounds by LC-ESI-MS/MS [32]. Multiple reaction monitoring transitions, the optimum collision energies, and retention times for each species, representative LC-ESI-MS/MS chromatograms of phenolic compounds, and calibration curves, and sensitivity properties of the method are previously detailed by Snoussi and colleagues in 2022 [30].

2.3. Synthesis of nanoparticles

Silver Nitrate ($AgNO_3$) was used for the reaction [33]. For the experiment, (*D. flabellifolia*)-AgNPs were prepared by the green method using the aqueous extract of *D. flabellifolia* (AEDF) at 80°C for 15 mn. In a typical reaction mixture, 100 mL of a 3 mM Silver Nitrate ($AgNO_3$) solution was put in a two-neck round bottom flask containing 197 mL of bi-distilled (BD) water. The resulting mixture was heated under reflux at 80°C and constant stirring. Once the set temperature was reached, 3 mL of the aqueous extract of *D. flabellifolia* were added. When the set temperature was reached again, the count of the duration of the reaction was started. Under the above conditions, the concentration of $AgNO_3$ in the reaction mixture was 1 mM and each 100 mL of the reaction mixture contains 1 mL of the AEDF.

2.4. Characterization of the obtained AgNPs

2.4.1. *Ultraviolet-Visible Spectroscopy*

The formation of AgNPs was confirmed by UV-Vis spectroscopy (UV-Vis). The Surface Plasmon Resonance

Fig. 1. *Ducrosia flabellifolia* plant body [31].

(SPR) is the characteristic property of silver, gold and some other metal nanoparticles. UV-Vis spectra were made using a Spectro UV-Vis Double Beam PC Scanning Spectrophotometer (Labomed UVD-2950, USA).

2.4.2. *Scanning Electron Microscopy (SEM)*

The morphology of the prepared (*D. flabellifolia*)-AgNPs was examined by using Field Emission Scanning Electron Microscope (SEM) (Thermo Scientific Quattro, Waltham, MA, USA). SEM imaging was performed under a high vacuum and samples (fragments of the prepared glass slide) were metalized with gold prior to characterization. SEM images were analyzed by using Image J software to measure the particle size and size distribution of the prepared AgNPs.

2.4.3. *X-Ray Diffraction (XRD)*

The identification of the crystalline structure of the prepared (*D. flabellifolia*)-AgNPs was made by using an X-Ray Diffractometer (Shimadzu, XRD-7000 with an X-ray wavelength Cu detector, Japan). The scanned 2 Theta ranges between 5 and 80 degrees.

2.5. Biological activities of the synthesized AgNPs

2.5.1. *Antimicrobial activities of (D. flabellifolia)-AgNPs*

Well diffusion assay was used for the determination of the diameter of growth inhibition zone estimated on agar medium (Mueller Hinton for bacteria and Sabouraud Chloramphenicol agar for *Candida* strains). This study includes 13 ESKAPE pathogens and 3 Candida species as listed in Table 1 below.

After incubation, the diameter of the growth inhibition zone (GIZ) was recorded for each bacterial and yeast strain and the mean diameter was calculated as the average of three records. All tests were done in triplicate. Ampicillin (10 UI) and amphotericin B (10 mg/mL) were used as control drugs.

Minimal inhibitory concentration (MICs) and minimal bactericidal/fungicidal concentration (MBC/MFC) were determined in liquid broth using microdilution assay. *D. flabellifolia*-AgNPs were tested at different concentrations ranging from 0.024 mg/mL to 2.5 mg/mL. The character of the tested solution was estimated by using the scheme proposed by Moroh and colleagues [34].

2.6. Anti-quorum sensing activities of *D. flabellifolia*-AgNPs

2.6.1. *Quorum sensing inhibition assay*

A well-diffusion assay was used to screen the anti-QS activity of different synthesized nanoparticles against *Chromobacterium violaceum* MTCC-2656, *Pseudomonas aeruginosa* MTCC-741, and *Serratia marcescens* MTCC-97 [35]. Briefly, overnight-grown culture of bacterial strain was streaked onto Lauria Bertani agar plates and wells were made with gel puncture. Following puncture of the wells, 50 µL of different synthesized nanoparticles were inoculated into the respective wells and the plates were incubated at 30°C for 24 h. An inhibitory effect of the indicator strain surrounding the well was considered a positive sign of QS interference.

2.6.2. *Determination of Minimum Inhibitory Concentration (MIC)*

In order to determine the MIC values of newly synthesized nanoparticles against different pathogenic bacteria such as *C. violaceum* MTCC-2656 (*C. violaceum*), *P. aeruginosa* MTCC-741, and *S. marcescens* MTCC-97, broth dilution method was used [36]. A series of double dilutions of different synthesized nanoparticles from 1000 µg/mL to 1.95 µg/mL concentrations were used in Mueller Hinton broth with an active bacterial culture. A control was prepared using only inoculated broth, which was incubated at 37 °C for 24 h. An MIC is defined as the lowest concentration that does not allow any visible growth on the tubes after the experiment.

2.7. Statistical analysis

All measurements will be carried out in triplicate and the results were presented as mean values ± SD (standard deviations). Statistical analyses will be performed using a one-way analysis of variance ANOVA test.

3. Results

Table 2 summarizes the identified compounds in *D. flabellifolia* boiled extract using ESI-MS/MS technique. Results showed the identification of twenty-three compounds dominated (mg/g of extract) by chlorogenic acid (5980.96±73.12), protocatechuic acid (5980.96±73.12), ferulic acid (112.43±1.541), caffeic acid (63.61±0.495), 2,5-dihydroxybenzoic acid (60.68±2.518), and gallic acid (43.96±0.251).

The reduction of Ag+ ions in the aqueous solution was made by the reducing phytochemicals present in the boiled aqueous extract from *D. flabellifolia* aerial parts. The reduction was visible from the color change of the solution (Fig. 2). The reaction mixture was colorless or pale yellow for the most concentrated solutions at the beginning of the reaction and turned gradually to brownish once the reduction started.

The kinetic of *D. flabellifolia*-AgNPs formation was followed by UV-Vis. It can be seen from Fig. 3 that the wavelength of maximum absorption (λmax) corresponds to the Surface Plasmon Resonance (SPR) of the prepared *D. flabellifolia*-AgNPs. The SPR was small for this

Table 1. ESKAPE pathogens and *Candida* species used in this study.

Code	ESKAPE pathogens
M2	*Escherichia coli* (212)
M6	*Escherichia coli* (215)
M7	*Enterococcus faecalis* (268)
M8	*Enterobacter cloacae* (235)
M9	*Enterobacter faecium* (260)
M10	*Acinetobacter baumannii* (248)
M11	*Staphylococcus hominis* (140 BC)
M12	*Staphylococcus aureus* (259)
M1	*Staphylococcus aureus* (217)
M13	*Staphylococcus epidermidis* (BC 161)
M14	*Klebsiella pneumoniae* (147)
M15	*Klebsiella pneumoniae* (280)
M16	*Pseudomonas aeruginosa* (249)
Code	***Candida* spp.**
A1	*Candida utilis* ATCC 9255
A8	*Candida tropicalis* ATCC 1362
A15	*Candida albicans* ATCC 20402

Table 2. Chemical composition of *D. flabellifolia* boiled aqueous extract by using ESI–MS/MS technique.

N°	Identified compounds	Retention Time (min)	Abondance (mg/Kg of extract)	Chemical Formula	Molecular Weight (g/mol)
1	Gallic acid	8.891	43.96±0.251	$C_7H_6O_5$	170.12
2	Protocatechuic acid	10.818	295.35±0.395	$C_7H_6O_4$	154.12
3	3,4-Dihydroxyphenylacetic acid	11.224	1.38±0..030	$C_8H_8O_4$	168.15
4	Pyrocatechol	11.506	9.66±0.054	$C_6H_6O_2$	110.11
5	Chlorogenic acid	11.802*	4154.16±16.353	$C_{16}H_{18}O_9$	354.31
6	2,5-Dihydroxybenzoic acid	12.412	60.68±2.518	$C_7H_6O_4$	154.12
7	4-Hydroxybenzoic acid	12.439	20.82±1.182	$C_7H_6O_3$	138.12
8	(-)-Epicatechin	12.458*	3.88±0.154	$C_{15}H_{14}O_6$	290.27
9	Caffeic acid	12.841	63.61±0.495	$C_9H_8O_4$	180.16
10	Syringic acid	12.963	25.19±0.196	$C_9H_{10}O_5$	198.17
11	3-Hydroxybenzoic acid	13.259	7.76±0.457	$C_7H_6O_3$	138.12
12	Vanillin	13.379	9.92±0.353	$C_8H_8O_3$	152.15
13	Sinapic acid	13.992	30.24±1.222	$C_{11}H_{12}O_5$	224.21
14	*p*-Coumaric acid	14.022	30.772±1.458	$C_9H_8O_3$	164.16
15	Ferulic acid	14.120	112.43±1.541	$C_{10}H_{10}O_4$	194.18
16	Luteolin 7-glucoside	14.266	3.87±0.392	$C_{21}H_{20}O_{11}$	448.4
17	Hyperoside	14.506*	4.59±0.101	$C_{21}H_{20}O_{12}$	464.4
18	Rosmarinic acid	14.600	4.34±0.135	$C_{18}H_{16}O_8$	360.3
19	2-Hydroxycinnamic acid	15.031	22.00±0.402	$C_9H_8O_3$	164.16
20	Pinoresinol	15.118	4.42±0.092	$C_{20}H_{22}O_6$	358.4
21	Eriodictyol	15.247	1.65±0.103	$C_{15}H_{12}O_6$	288.25
22	Quercetin	15.668	1.99±0.335	$C_{15}H_{10}O_7$	302.23
23	Kaempferol	16.236	1.48±0.067	$C_{15}H_{10}O_6$	286.23

*: Compounds identified by positive Ionization mode

concentration at the beginning of the reaction. The λmax was around 430 nm–440 nm for the first twenty minutes.

Image J software was used to analyze SEM micrographs, in order to measure the particle size and thus the size distribution. In fact, more than one hundred nanoparticles were measured, and the size distribution was calculated automatically by the software. Results from SEM image analysis revealed that the shape of the newly synthetized *D. flabellifolia*-AgNPs was almost spherical with an average particle size of 16.961±2.914 nm (Fig. 4).

The XRD patterns are shown in Figure 5. The diffraction peaks were as follows, 2θ = 27.75°, 32.16°, 38.05°, 44.14°, 46.15°, 54.72°, 57.49°, 64.40°, 67.27°, 74.20°, 77.26° and 77.48°. The following peaks, 38.05°, 44.14°, 64.40°, and 77.26° were assigned to the planes (111), (200), (220) and (311) corresponding to a cubic lattice of silver (Reference code: 00-004-0783, ICSD 64706 (PDF 87-597)). The following peaks 27.75°, 32.16°, 46.15°, 54.72°, 57.49°, 67.27°, 74.20°, and 77.48° were assigned to the planes (111), (200), (220), (311), (222), (400), (331), and (420) corresponding to a cubic lattice of silver chloride (Reference code: 01-085-1355, ICSD 064734 (PDF 31-1238)). The prepared nanoparticles are composed mostly of AgNPs (86%) and AgCl NPs (14%).

The newly synthesized *D. flabellifolia*-AgNPs were tested for their ability to inhibit the growth of twelve ESKAPE pathogens and four *Candida* species. Results are summarized in Table 3 below. Overall, the newly synthesized nanoparticles were able to inhibit the growth of all tested ESKAPE pathogens and *Candida* species with different degrees and in a concentration-dependent manner.

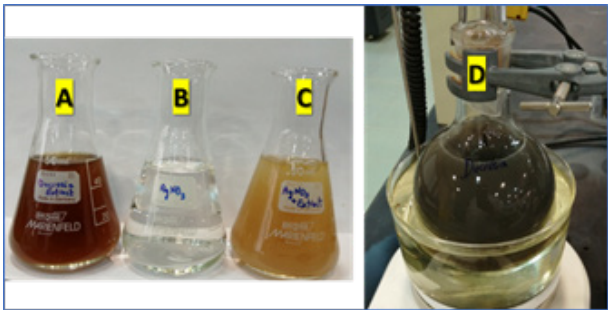

Fig. 2. Color change of the reaction mixture maintained at 80°C after 70 min. (A): *D. flabellifolia* filtered. extract, (B): $AgNO_3$ solution, (C): mixture of *D. flabellifolia* and silver nitrate solution, and (D): reaction mixture after 70 mn.

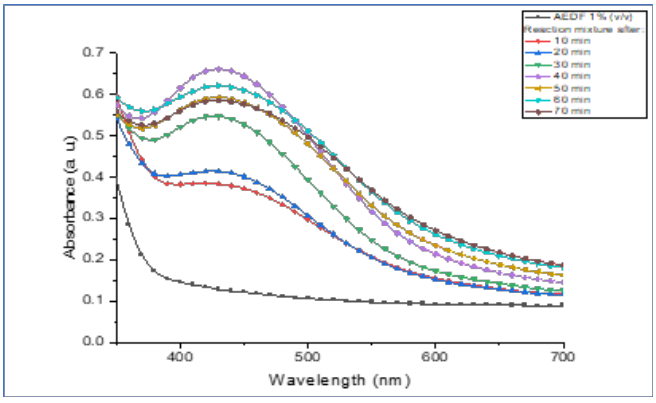

Fig. 3. UV-Vis absorption spectra of the *D. flabellifolia*-AgNPs and the reaction mixture (DFAE 1% (v/v) / 1 mM $AgNO_3$) after different reaction times at 80°C.

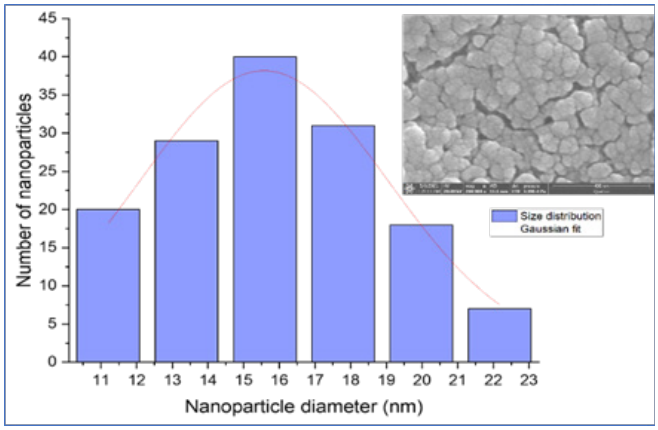

Fig. 4. Size distribution histogram and Gaussian fitting of the newly synthesized *D. flabellifolia*-AgNPs determined from SEM micrographs by using Image J software.

In fact, the highest mean growth inhibition zones (mGIZ) were obtained at 5 mg/mL of *D. flabellifolia*-AgNPs ranging from 15.33±0.57 mm (For *Staphylococcus aureus*, 217) to 33.67±1.15 mm (For *P. aeruginosa*, 249). The obtained mGIZ of *D. flabellifolia*-AgNPs at 1mg/mL, 2.5 mg/mL, and 5 mg/mL were higher than those of the standard antibiotic used (Ampicillin) for all tested bacteria, highlighting high antimicrobial activities of the newly synthetized *D. flabellifolia*-AgNPs.

Using microdilution assay, results have shown that *D. flabellifolia*-AgNPs were able to inhibit the growth of all tested ESKAPE pathogens at low concentrations ranging from 0.078 mg/mL (For *P. aeruginosa*) to 0.312 mg/mL (For *K. pneumoniae*, *S. epidermidis*, *E. cloacae*, and *E. coli*). Concentrations as low as 0.312 mg/mL of the newly synthetized *D. flabellifolia*-AgNPs are sufficient to kill all tested ESKAPE pathogens. The *D. flabellifolia*-AgNPs exhibited bactericidal profile against all tested ESKAPE pathogens with MBC/MIC ratio lower than 4. Moreover, MICs and MBCs values of *D. flabellifolia*-AgNPs were lower than the reference drug used (Ampicillin).

In addition, *D. flabellifolia*-AgNPs are less active against the tested *Candida* species with MICs of about 0.312 mg/mL, and MFCs values of about 5 mg/mL. The newly synthetized *D. flabellifolia*-AgNPs exhibited fungistatic profile, while the reference drug used has fungicidal action against all Candida species tested (Table 4).

3.1. Anti-QS activity

As part of the initial evaluation of the anti-QS activity of *D. flabellifolia*-AgNPs, their ability to modulate the QS activity of *C. violaceum, P. aeruginosa* and *S. marcescens* was examined *in-vitro*. An inhibitory effect of the indicator strain surrounding the well was considered a positive sign of QS interference. Results are presented in Fig. 6. To find out the antibacterial activity of *D. flabellifolia*-AgNPs against different pathogenic bacteria, a broth microdilution method was performed to determine the value of MIC. Results have shown that *D. flabellifolia*-AgNPs are able to inhibit *C. violaceum*, *P. aeruginosa*, and *S. marces-*

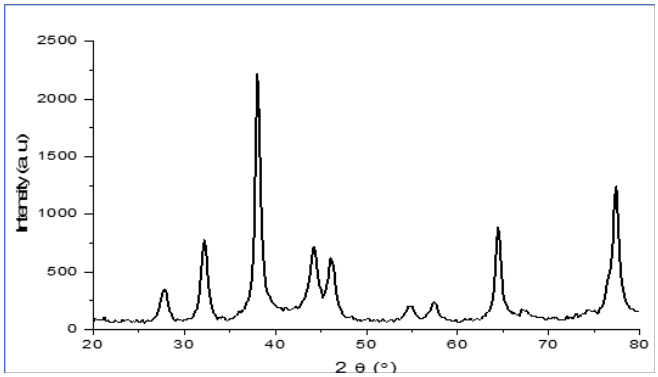

Fig. 5. PXRD diffractogram of the newly synthesized *D. flabellifolia*-AgNPs.

Table 3. Anti-ESKAPE and anti-*Candida* spp. activities of *D. flabellifolia*-AgNPs tested at three concentrations using well diffusion assay.

Code	Bacterial Strain	*D. flabellifolia*-AgNPs			Ampicillin mGIZ ±SD
		mGIZ at 1 mg/mL	mGIZ at 2.5 mg/mL	mGIZ at 5 mg/ml	
M2	*Escherichia coli* (212)	13.33±1.15	15.67±0.57	19.00±1.00	6.00±0.00
M6	*Escherichia coli* (215)	12.67±0.57	14.33±0.57	17.00±1.00	6.00±0.00
M7	*Enterococcus faecalis* (268)	15.00±1.00	16.67±0.57	29.00±1.73	6.00±0.00
M8	*Enterobacter cloacae* (235)	11.33±1.15	15.67±0.57	20.67±0.57	6.00±0.00
M9	*Enterobacter faecium* (260)	12.33±0.57	17.33±0.57	27.67±0.57	6.00±0.00
M10	*Acinetobacter baumannii* (248)	14.33±0.57	16.33±1.15	22.33±0.57	10.33±0.57
M11	*Staphylococcus hominis* (140 BC)	12.67±0.57	16.33±0.57	22.67±0.57	10.33±0.57
M12	*Staphylococcus aureus* (259)	16.00±0.00	19.67±0.57	25.00±0.00	6.00±0.00
M1	*Staphylococcus aureus* (217)	12.33±0.57	13.67±0.57	15.33±0.57	14.00±0.00
M13	*Staphylococcus epidermidis* (BC 161)	21.33±1.15	25.00±1.00	28.67±1.15	24.00±1.00
M14	*Klebsiella pneumoniae* (147)	15.00±1.00	20.67±0.57	23.67±0.57	6.00±0.00
M15	*Klebsiella pneumoniae* (280)	12.67±0.57	14.67±1.15	18.67±1.15	6.00±0.00
M16	*Pseudomonas aeruginosa* (249)	26.67±1.55	30.33±0.57	33.67±1.15	6.00±0.00
Code	**Yeasts and molds**	**mGIZ at 1 mg/mL**	**mGIZ at 2.5 mg/mL**	**mGIZ at 5 mg/ml**	**Amphotericin B GIZ ±SD**
A1	*Candida utilis* ATCC 9255	6.00±0.00	6.00±0.00	12.67±0.57	11.67±0.57
A8	*Candida tropicalis* ATCC 1362	6.00±0.00	6.00±0.00	12.67±0.57	14.33±0.57
A15	*Candida albicans* ATCC 20402	6.00±0.00	6.00±0.00	13.33±1.15	12.67±0.57

Table 4. Determination of MICs, MBCs, and MFCs values of *D. flabellifolia*-AgNPs tested against twelve ESKAPE and four Candida spp. strains using microdilution assay.

Code	ESKAPE pathogens	*D. flabellifolia*-AgNPs			Ampicillin		
		MIC	MBC	MBC/MIC ratio	MIC	MBC	MBC/MIC ratio
M2	*Escherichia coli* (212)	0.156	0.625	4; Bactericidal	1.25	5	4; Bactericidal
M6	*Escherichia coli* (215)	0.3125	0.625	2; Bactericidal	1.25	5	4; Bactericidal
M7	*Enterococcus faecalis* (268)	0.156	0.325	2; Bactericidal	0.312	2.5	8; Bacteriostatic
M8	*Enterobacter cloacae* (235)	0.3125	0.625	2; Bactericidal	0.625	1.25	2; Bactericidal
M9	*Enterobacter faecium* (260)	0.156	0.312	2; Bactericidal	0.625	5	8; Bacteriostatic
M10	*Acinetobacter baumannii* (248)	0.156	0.625	4; Bactericidal	1.25	5	4; Bactericidal
M11	*Staphylococcus hominis* (140 BC)	0.156	0.625	4; Bactericidal	0.625	1.25	2; Bactericidal
M12	*Staphylococcus aureus* (259)	0.156	0.625	4; Bactericidal	0.625	1.25	2; Bactericidal
M1	*Staphylococcus aureus* (217)	0.156	0.625	4; Bactericidal	0.625	5	8; Bacteriostatic
M13	*Staphylococcus epidermidis* (BC 161)	0.3125	0.625	2; Bactericidal	0.312	0.625	2; Bactericidal
M14	*Klebsiella pneumoniae* (147)	0.3125	0.625	2; Bactericidal	0.625	5	8; Bacteriostatic
M15	*Klebsiella pneumoniae* (280)	0.156	0.625	4; Bactericidal	0.625	5	8; Bacteriostatic
M16	*Pseudomonas aeruginosa* (249)	0.078	0.625	8; Bactericidal	2.5	5	2; Bactericidal
Code	***Candida* spp.**	***D. flabellifolia*-AgNPs**			**Amphotericin B**		
		MIC	MFC	MFC/MIC ratio	MIC	MFC	MFC/MIC ratio
A1	*Candida utilis* ATCC 9255	0.3125	5	16; Fungistatic	0.78	1.56	2; Fungicidal
A8	*Candida tropicalis* ATCC 1362	0.3125	5	16; Fungistatic	0.195	0.78	4; Fungicidal
A15	*Candida albicans* ATCC 20402	0.3125	5	16; Fungistatic	0.195	0.39	2; Fungicidal

cens at 125 µg/mL.

4. Discussion

In this study, we report for the first time the synthesis, characterization, antimicrobial, and anti-quorum sensing activities of silver nitrate nanoparticles by using boiled extract from *D. flabellifolia* aerial parts. The study of the phytochemical profile of the boiled aqueous extract revealed the identification of 23 molecules, mainly chlorogenic acid, protocatechuic acid, ferulic acid, caffeic acid, 2,5-dihydroxybenzoic acid, and gallic acid. Similar results have discussed the chemical composition of *D. flabellifolia* from Egypt, Jordan, Iran, and Saudi Arabia [30, 31; 37-41]. In fact, we have reported the identification of twenty phytocompounds in the methanol/water extract from *D. flabellifolia* aerial parts collected from Hail region (Saudi Arabia) where chlorogenic acid (5980.96 ± 73.12 mg/g of extract), ferulic acid (180.58 ± 2.77 mg/g of extract), caffeic acid (70.90 ± 1.75 mg/g of extract), and sinapic acid (61.74 ± 2.79 mg/g of extract) were the main compounds. In addition, our team has reported the identification of decanal and dodecanal as main compounds in *D. flabellifolia* essential oil collected from arid sandy soil in Hail (Saudi Arabia), and farnesyl pyrophosphate, methyl 7-desoxypurpurogallin-7-carboxylate trimethyl ether, dihydro-obliquin, gummiferol, 2-phenylaminoadenosine, and 2,4,6,8,10-dodecapentaenal, as dominant compounds in the methanolic extract of the same plant species [31].

The newly synthesized *D. flabellifolia*-AgNPs were visualized by SEM and analyzed by Image J software and are spherical with an average nanoparticles size about 16.961±2.914 nm. After 70 min of boiling at 80°C. The formation of brown final color of the reaction mixture within 70 mn indicates the reduction of Ag+ ion ton Ag0 indicates the green synthesis of *D. flabellifolia*-AgNPs in the solution. It was previously reported that the appearance of brown color in the reaction mixture of AgNPs solution

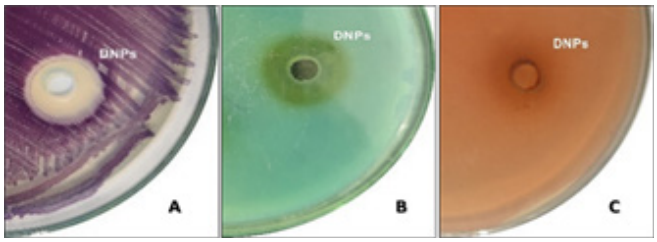

Fig. 6. *In-vitro* inhibition of *C. violaceum* (A), *P. aeruginosa* (B), and *S. marcescens* (C) by *D. flabellifolia*-AgNPs.

was due to the excitation of surface plasmon vibrations [42]. Moreover, the formation of *D. flabellifolia*-AgNPs was confirmed by ultraviolet-visible spectroscopy technique, with a maximum surface plasmon resonance (SPR) absorption band between 430 nm–440 nm at 80°C. Few studies have reported the synthesis of silver nanoparticles using *Ducrosia* plant species extracts. In fact, using *D. anethifolia* extract, Amin and colleagues successfully synthesized spherical silver nanoparticles with a size range between 4 and 42.13 nm [43]. The average size of our *D. flabellifolia*-AgNPs was about 16.961±2.914 nm, closely related to the average size reported by Amin and colleagues [43] for *D. anethifolia*-AgNPs (11.4 nm). Similarly, using the same plant species (*D. anethifolia*), Darvish and colleagues [44] succeeded in synthesizing silver nitrate nanoparticles with a maximum absorbance at 460 nm and side distribution in the range of 3.02 to 20.8 nm (Average size 9.41 nm).

In this study, we report that green synthesized silver nanoparticles from *D. flabellifolia* aqueous extract were able to inhibit the growth of several pathogenic bacteria, mainly ESKAPE microorganisms with low MICs and MBCs values. In fact, our results that *D. flabellifolia* silver nanoparticles exhibited high to very high anti-ESKAPE activity with mean growth inhibition zone higher than 11

to 20 mm as defined by Parveen and colleagues [43]. In addition, our results showed that the MICs values ranged from 78 to 312 µg/mL, and MBCs values from 312 to 625 µg/mL. While, against *Candida* species, *D. flabellifolia*-AgNPs were active at MIC value of about 321 µg/mL, and MFC value about 5 mg/mL. Similar results were reported by Amin and colleagues [44] who found that *D. anethifolia* silver nanoparticles were effective against *S. aureus* ATCC 29933, *E. faecalis* ATCC 51299, *E. coli* 25922, and *P. aeruginosa* ATCC 27853 at MICs values ranging from 32 to 128 µg/mL. Darvish and colleagues [45] reported that spherical silver nanoparticles synthesized using *D. anethifolia* aqueous extract were able to attenuate the viability of MCF-7 and MDA-MB-231 cell lines using the MTT technique in a time-dependent and concentration-dependent manner. In fact, the calculated inhibitory concentration of *D. anethifolia*-AgNPs (IC_{50} 72h) after 72 h was estimated at about 16.87±2.76 µg/mL against MDA-MB-231 cell lines, and about 27.9±2.06 µg/mL about MCF-7 cell lines.

Previous results have reported the green synthesis of silver nanoparticles by using plant species and their waste material [33; 46-48]. It has been reported that silver nanoparticles synthesized by using extracts from plants, fungi, bacteria, actinomycetes, and algae (Red, blue, green, and brown) are active against large collection of Gram-positive and Gram-negative bacteria including *Bacillus subtilis*, *S. aureus*, *P. aeruginosa*, *B. cereus*, *Salmonella typhimurium*, *E. coli*, *Vibrio fluvialis*, *V. damsela*, *Proteus mirabilis*, *K. pneumoniae*, methicillin-resistant *S. aureus*, and *Micrococcus luteus* [49]. More recently, Merghni and colleagues reported the green synthesis of silver nanoparticles by using dried orange peel extract with high antagonist activities against methicillin-resistant *S. aureus* strains with inhibition zones between 12 and 14 mm and MICs values between 1.56 and 12.5 µg/mL. The same authors reported that orange peel-AgNPs were able to disrupt the mature biofilm formed by MRSA strains on polystyrene microtiter plates. In addition, many researchers have reported the effectiveness of plant silver nanoparticles in combating ESKAPE pathogens [49-54]. In fact, Musthafa and colleagues [52] reported the new synthesis of spherical Ag-NPs using *Picrorhiza kurroa* plant extracts able to inhibit the growth of *E. coli*, *K. pneumonia*, *P. aeruginosa*, *S. aureus*, *A. baumannii* and *E. aerogenes* with growth inhibition zones ranging from 8 to 20 mm. More recently, Raza and colleagues reported that AgNPs synthesized using tea extracts have high antibacterial properties against ESKAPE pathogens causing approximately 80% bacterial cell death in within only three hours at a concentration of 0.1 mg/ mL as compared to ampicillin.

We report also in this study that the newly synthetized *D-flabellifolia* AgNPs were able to inhibit cell to cell communication in *C. violaceum*, *P. aeruginosa*, and *S. marcescens* at 125 µg/mL. Previous results have shown that silver nitrate nanoparticles synthetized by using *Vetiveria zizanioides* root extract were able to inhibit many virulence factors in *S. marcescens* controlled by the quorum sensing system like the production of prodigiosin, protease, lipase, and exopolysaccharide, and biofilm formation without inhibiting its growth [55]. Similarly, newly synthesized silver nanoparticles using piper betle aqueous extract were able to attenuate the production of QS-mediated virulence factors by uropathogenic bacteria like *Proteus mirabilis*, *P. aeruginosa*, *E. coli*, and *S. marcescens* [56]. Recently, Qais and colleagues [57] reported that silver nanoparticles synthesized using aqueous extract from *Carum copticum* were able to inhibit violacein production in *C. violaceum*, the production of pyoverdine, proteases, elastases, rhamnolipid, and motility in *P. aeruginosa*, and prodigiosin, proteases, and motility in *S. marcescens*. *In silico* approaches highlighted that AgNPs could bind to LasI synthase, RhlI synthase, and transcriptional receptor protein LasR and RhlR of the two *P. aeruginosa* Las and Rhl quorum sensing systems [58]. Similar results are reported with selenium nanoparticles [59], and silver, zinc oxide, and copper oxide nanoparticles [60].

5. Conclusion

Overall, the newly synthesized nanoparticles using aqueous extract from *D. flabellifolia* aerial parts showed a spherical shape with low particle size. The obtained extract was dominated by phytoconstituents with promising biological activities. Results showed that *D. flabellifolia* silver nanoparticles were able to interfere with the quorum sensing systems in *P. aeruginosa*, *C. violaceum*, and *S. marcescens* bacteria. Similarly, the newly synthesized silver nanoparticles possessed potent anti-ESKAPE activities. The results highlight the possible use of silver nitrate nanoparticles synthesized using *D. flabellifolia* extract as an alternative solution to combat multidrug-resistant microorganisms and to attenuate their virulence.

Acknowledgments

This research has been funded by the Scientific Research Deanship at the University of Ha'il – Saudi Arabia through project number RG-21 113.

Funding

The authors thank the Scientific Research Deanship at the University of Ha'il for funding this project through project number RG-21113.

Conflict of interest

The authors declare no conflict of interest.

References

1. Venkateswaran P, Vasudevan S, David H, Shaktivel A, Shanmugam K, Neelakantan P, Solomon AP. Revisiting ESKAPE Pathogens: virulence, resistance, and combating strategies focusing on quorum sensing. Front Cell Infect Microbiol 2023; 13:1159798. http://dx.doi.org/10.3389/fcimb.2023.1159798.
2. Cella E, Giovanetti M, Benedetti F, Scarpa F, Johnston C, Borsetti A, Ceccarelli G, Azarian T, Zella D, Ciccozzi M. Joining Forces against Antibiotic Resistance: The One Health Solution. Pathogens 2023; 12, 1074. http://dx.doi.org/10.3390/pathogens12091074.
3. Frieri M, Kumar K, Boutin A. Antibiotic resistance. J Infect Public Health 2017; 10, 369-378. http://dx.doi.org/10.1016/j.jiph.2016.08.007.
4. Mukuna W, Aniume T, Pokharel B, Khwatenge C, Basnet A, Kilonzo-Nthenge A. Antimicrobial susceptibility profile of pathogenic and commensal bacteria recovered from cattle and goat farms. Antibiotics 2023; 12, 420. http://dx.doi.org/10.3390/antibiotics12020420.
5. Manaia CM. Assessing the Risk of Antibiotic Resistance transmission from the environment to humans: non-direct proportionality between abundance and risk. Trends Microbiol 2017; 25, 3.

http://dx.doi.org/10.1016/j.tim.2016.11.014.
6. Almatroudi A. Silver nanoparticles: synthesis, characterisation and biomedical applications. Open Life Sciences 2020;15(1):819-839. http://dx.doi.org/10.1515/biol-2020-0094.
7. Lee SH, Jun B-H. Silver Nanoparticles: Synthesis and Application for Nanomedicine. Int J Mol Sci 2019; 20(4):865. .
8. Bilal M, Rasheed T, Iqbal HMN, Hu H, Zhang X. Silver nanoparticles: Biosynthesis and antimicrobial potentialities. Int J Pharmacol 2017; 13: 832-845. http://dx.doi.org/10.3923/ijp.2017.832.845.
9. Ashraf SA, Siddiqui AJ, Elkhalifa AEO, Khan MI, Patel M, Alreshidi M, Moin A, Singh R, Snoussi M, Adnan M. Innovations in nanoscience for the sustainable development of food and agriculture with implications on health and environment. Sci Total Environ 2021; 768,144990. http://dx.doi.org/10.1016/j.scitotenv.2021.144990.
10. Rittner MN, Abraham T. Nanostructured materials: An overview and commercial analysis. The Journal of The Minerals, Metals & Materials Society 1998; 50,37-38. http://dx.doi.org/10.1007/s11837-998-0065-4.
11. Gahlawat G, Choudhury AR. A review on the biosynthesis of metal and metal salt nanoparticles by microbes. RSC Adv 2019; 9(23):12944-12967. http://dx.doi.org/10.1039/c8ra10483b.
12. Ibrahim Khan I, Saeed K, Khan I. Nanoparticles: Properties, applications and toxicities. Arab J Chem 2020; 12: 908-931. http://dx.doi.org/10.1016/j.arabjc.2017.05.011.
13. Austin LA, Mackey MA, Dreaden EC, El-Sayed MA. The optical, photothermal, and facile surface chemical properties of gold and silver nanoparticles in biodiagnostics, therapy, and drug delivery. Arch Toxicol 2014; 88:1391-1417. http://dx.doi.org/10.1007/s00204-014-1245-3.
14. Majdalawieh A, Kanan MC, El-Kadri O, Kanan SM. Recent advances in gold and silver nanoparticles: synthesis and applications. J Nanosci Nanotechnol 2014;14:4757-4780. http://dx.doi.org/10.1166/jnn.2014.9526.
15. Prasad R, Pandey R, Barman I. Engineering tailored nanoparticles with microbes: quo vadis? Wiley Interdiscip Rev Nanomed Nanobiotechnol 2016;8(2):316-30. http://dx.doi.org/10.1002/wnan.1363.
16. Aritonang HF, Koleangan H, Wuntu AD. Synthesis of Silver Nanoparticles Using Aqueous Extract of Medicinal Plants' (Impatiens balsamina and Lantana camara) Fresh Leaves and Analysis of Antimicrobial Activity. Int J Microbiol 2019; 2019:8642303. http://dx.doi.org/10.1155/2019/8642303.
17. Syafiuddin A, Salmiati Salim MR, Kueh ABH, Hadibarata T, Nur H. A Review of silver nanoparticles: Research trends, global consumption, synthesis, properties, and future Challenges. J Chin Chem Soc 2017; 64: 732-756. http://dx.doi.org/10.1002/jccs.201700067.
18. Desireddy A, Conn BE, Guo J, Yoon B, Barnett RN, Monahan BM, Kirschbaum K, Griffith WP, Whetten RL, Landman U, Bigioni TP. Ultrastable silver nanoparticles. Nature 2013; 501:399-402. http://dx.doi.org/10.1038/nature12523.
19. Ashanrani PV, Mun LK, Hande G, Valiyaveettil MPS. Cytotoxicity and genotoxicity of silver nanoparticles in human cells. ACS Nano 2009; 3: 279-290. http://dx.doi.org/10.1021/nn800596w.
20. Vazquez-Muñoz R, Borrego B, Juárez-Moreno K, García-García M, Mota Morales JD, Bogdanchikova N, Huerta-Saquero A. Toxicity of silver nanoparticles in biological systems: Does the complexity of biological systems matter? Toxicol Lett 2017; 276:11-20. http://dx.doi.org/10.1016/j.toxlet.2017.05.007.
21. Santajit S, Indrawattana N. Mechanisms of Antimicrobial Resistance in ESKAPE Pathogens. Biomed Res Int 2016; 1-8. http://dx.doi.org/10.1155/2016/2475067.
22. Van Melderen L, DeBast MS. Bacterial toxin–antitoxin systems: more than selfish entities?. PLoS Genetics 2009; 5(3), e1000437. http://dx.doi.org/10.1371/journal.pgen.1000437.
23. Pendleton JN, Gorman SP, Gilmore BF. Clinical relevance of the ESKAPE pathogens. Expert Rev Anti Infect Ther 2013; 11(3):297-308. http://dx.doi.org/10.1586/eri.13.12.
24. Marturano JE, Lowery TJ. ESKAPE Pathogens in Bloodstream Infections Are Associated With Higher Cost and Mortality but Can Be Predicted Using Diagnoses Upon Admission. Open Forum Infect Dis 2019; 6(12): ofz503. http://dx.doi.org/10.1093/ofid/ofz503.
25. Schultz F, Anywar G, Tang H, Chassagne F, Lyles JT, Garbe L-A, Quave CL. Targeting ESKAPE pathogens with anti-infective medicinal plants from the Greater Mpigi region in Uganda. Sci Rep 2020;10: 11935. http://dx.doi.org/10.1038/s41598-020-67572-8.
26. Al Marjani FM, Hasan RN, Khadam ZA, Al-Saryi NA, Al Rahhal AH. ESKAPE Bacteria and Antimicrobial resistance. Palarch's Journal Of Archaeology Of Egypt/Egyptology 2020; 17(7):7585-7606.
27. Prasher P, Singh M, Mudila H. (2018). Silver nanoparticles as antimicrobial therapeutics: current perspectives and future challenges. 3 Biotech. 8(10):411. http://dx.doi.org/10.1007/s13205-018-1436-3.
28. Adil M, Khan T, Aasim M, Khan AA, Ashraf M. Evaluation of the antibacterial potential of silver nanoparticles synthesized through the interaction of antibiotic and aqueous callus extract of *Fagonia indica*. AMB Expr 2019; 9: 75. http://dx.doi.org/10.1186/s13568-019-0797-2.
29. Mseddi K, Alimi F, Noumi E, Veettil VN, Deshpande S, Adnan M, Hamdi H, Elkahoui S, Alghamdi A, Kadri A, Patel M, Snoussi M. Thymus musilii Velen. as a promising source of potent bioactive compounds with its pharmacological properties: In vitro and in silico analysis, Arab J Chem 2020; 13(8):6782-6801. http://dx.doi.org/10.1016/j.arabjc.2020.06.032.
30. Snoussi M, Ahmad I, Aljohani AMA, Patel H, Abdulhakeem MA, Alhazmi YS, Tepe B, Adnan M, Siddiqui AJ, Sarikurkcu C, Riadh B, Feo V, Alreshidi M, Noumi E. Phytochemical Analysis, Antioxidant, and Antimicrobial Activities of *Ducrosia flabellifolia*: A Combined Experimental and Computational Approaches. Antioxidants (Basel). 2022;11(11):2174. http://dx.doi.org/10.3390/antiox11112174.
31. Snoussi M, Lajimi RH, Badraoui R, Al-Reshidi M, Abdulhakeem MA, Patel M, Siddiqui AJ, Adnan M, Hosni K, De Feo V, Polito F, Kadri A, Noumi E. Chemical Composition of *Ducrosia flabellifolia* L. Methanolic Extract and Volatile Oil: ADME Properties, In Vitro and In Silico Screening of Antimicrobial, Antioxidant and Anticancer Activities. Metabolites 2022;13(1):64. http://dx.doi.org/10.3390/metabo13010064.
32. Cittan M, Çelik A. Development and validation of an analytical methodology based on Liquid Chromatography–Electrospray Tandem Mass Spectrometry for the simultaneous determination of phenolic compounds in olive leaf extract. J Chromatogr Sci 2018, 56, 336-343. http://dx.doi.org/10.1093/chromsci/bmy003.
33. Merghni A, Lassoued MA, Noumi E, Hadj Lajimi R, Adnan M, Mastouri M, Snoussi M. Cytotoxic Activity and Antibiofilm Efficacy of Biosynthesized Silver Nanoparticles against Methicillin-Resistant Staphylococcus aureus Strains Colonizing Cell Phones. Can J Infect Dis Med Microbiol. 2022; 2022: 9410024. http://dx.doi.org/10.1155/2022/9410024.
34. Moroh JL, Bahi C, Dje K, Loukou YG, Guide Guina F. Etude de l'activité antibactérienne de l'extrait acétatique de Morinda morindoides (Baker) Milne-Redheat (Rubiaceae) sur la croissance in vitro des souches d'*Escherichia coli*. Bull Soc R Sci Liege 2008; 77:44–61. http://dx.doi.org/10.1007/s10298-011-0612-y.

35. Zahin M, Hasan S, Aqil F, Khan M, Ahmad S, Husain FM, Ahmad I. Screening of certain medicinal plants from India for their anti-quorum sensing activity. Indian J Exp Biol 2010;48(12):1219-24.
36. CLSI (2014). Performance Standards for Antimicrobial Susceptibility Testing; Twenty-Fourth Informational Supplement. Twenty-Fourth Informational Supplement. Wayne, PA: Clinical and Laboratory Standards Institute.
37. Al-Ghamdi FA; Abdelwahab AT. Volatile oil composition from stems, leaves and flowers of Ducrosia flabellifolia Boiss. From northern border of Saudi Arabia. Int. J Appl Biol Pharm Technol. 2014; 5, 296-300.
38. Talib WH; Issa RA; Kherissat F; Mahasne AM. Jordanian Ducrosia flabellifolia inhibits proliferation of breast cancer cells by inducing apoptosis. Br J Med Med Res 2013; 3, 771-783. http://dx.doi.org/10.9734/bjmmr/2013/3077.
39. Shahabipour S, Firuzi O, Asadollahi M, Faghihmirzaei E, Javidnia K. Essential oil composition and cytotoxic activity of Ducrosia anethifolia and Ducrosia flabellifolia from Iran. J Essent Oil Res 2013; 25, 160-163. http://dx.doi.org/10.1080/10412905.2013.773656.
40. Mottaghipisheh J, Boveiri Dehsheikh A, Mahmoodi Sourestani M, Kiss T, Hohmann J, Csupor D. *Ducrosia* spp., Rare Plants with Promising Phytochemical and Pharmacological Characteristics: An Updated Review. Pharmaceuticals 2020; 13, 175. http://dx.doi.org/10.3390/ph13080175.
41. Al-Shudiefat M, Al-Khalidi K, Abaza I, Afifi FU. Chemical composition analysis and antimicrobial screening of the essential oil of a rare plant from Jordan: *Ducrosia flabellifolia*. Anal Lett 2013; 47, 422-432. http://dx.doi.org/10.1080/00032719.2013.841176.
42. Hamouda RA, Hussein MH, Abo-Elmagd RA, Bawazir SS. Synthesis and biological characterization of silver nanoparticles derived from the cyanobacterium *Oscillatoria limnetica*. Sci Rep 9(1):13071, 2019. http://dx.doi.org/10.1038/s41598-019-49444-y.
43. Amin M, Kouhbanani J, Beheshtkhoo N, Nasirmoghadas P. Green synthesis of spherical silver nanoparticles using Ducrosia anethifolia aqueous extract and its antibacterial activity. J Environ Treat Tech 2019; 7:461–466.
44. Darvish S, Kahrizi MS, Özbolat G, Khaleghi F, Mortezania Z, Sakhaei D. Silver nanoparticles: biosynthesis and cytotoxic performance against breast cancer MCF-7 and MDA-MB-231 cell lines. Nanomed Res J 2022; 7(1): 83-92. http://dx.doi.org/ 10.22034/NMRJ.2022.01.008.
45. Parveen M, Ghalib RM, Khanam Z, Mehdi SH, Ali M. A Novel antimicrobial agent from the leaves of Peltophorum vogelianum (Benth.) Nat Prod Res 2010; 24:1268–1273. http://dx.doi.org/10.1080/14786410903387688.
46. Alshahrani MY, Rafi Z, Alabdallah NM, Shoaib A, Ahmad I, Asiri M, Zaman GS, Wahab S, Saeed M, Khan S. A Comparative Antibacterial, Antioxidant, and Antineoplastic Potential of Rauwolfia serpentina (L.) Leaf Extract with Its Biologically Synthesized Gold Nanoparticles (R-AuNPs). Plants 2021; 10, 2278. http://dx.doi.org/10.3390/plants10112278.
47. Oves M, Ahmar Rauf M, Aslam M, Qari HA, Sonbol H, Ahmad I, Sarwar Zaman G, Saeed M. Green synthesis of silver nanoparticles by *Conocarpus lancifolius* plant extract and their antimicrobial and anticancer activities. Saudi J Biol Sci 2022;29(1):460-471. http://dx.doi.org/10.1016/j.sjbs.2021.09.007.
48. Siddiqui AJ, Kumari N, Adnan M, Kumar S, Abdelgadir A, Saxena J, Badraoui R, Snoussi M, Khare P, Singh R. Impregnation of Modified Magnetic Nanoparticles on Low-Cost Agro-Waste-Derived Biochar for Enhanced Removal of Pharmaceutically Active Compounds: Performance Evaluation and Optimization Using Response Surface Methodology. Water 2023; 15, 1688. http://dx.doi.org/10.3390/w15091688.
49. Roy A, Bulut O, Some S, Mandal AK, Yilmaz MD. Green synthesis of silver nanoparticles: biomolecule-nanoparticle organizations targeting antimicrobial activity. RSC Adv 2019; 9, 2673-2702. http://dx.doi.org/10.1039/c8ra08982e.
50. Rai MK, Deshmukh SD, Ingle AP, Gade AK. Silver nanoparticles: the powerful nanoweapon against multidrug-resistant bacteria. J Appl Microbiol. 2012;112(5):841-52. http://dx.doi.org/10.1111/j.1365-2672.2012.05253.x.
51. Radzig MA, Nadtochenko VA, Koksharova OA, Kiwi J, Lipasova VA, Khmel IA. Antibacterial effects of silver nanoparticles on gram-negative bacteria: influence on the growth and biofilms formation, mechanisms of action. Colloids Surf B Biointerfaces. 2013; 102:300-6. http://dx.doi.org/10.1016/j.colsurfb.2012.07.039.
52. Musthafa M, Gobianand K, Manohar M. Anti-ESKAPE activity of green synthesized silver nanoparticles from Picrorhiza kurroa Royle ex Benth. IJPSR 2020; 11(10):5004-5009. http://dx.doi.org/10.1007/springerreference_69127.
53. Khan MH, Unnikrishnan S, Ramalingam K. Antipathogenic Efficacy of Biogenic Silver Nanoparticles and Antibiofilm Activities Against Multi-drug-Resistant ESKAPE Pathogens. Appl Biochem Biotechnol 2023; Jul 18. doi: 10.1007/s12010-023-04630-7. http://dx.doi.org/10.1007/s12010-023-04630-7.
54. Raza S, Wdowiak M, Grotek M, Adamkiewicz W, Nikiforow K, Mente P, Paczesny J. Enhancing the antimicrobial activity of silver nanoparticles against ESKAPE bacteria and emerging fungal pathogens by using tea extracts. Nanoscale Adv 2023;5(21):5786-5798. http://dx.doi.org/10.1039/d3na00220a.
55. Ravindran D, Ramanathan S, Arunachalam K, Jeyaraj GP, Shunmugiah KP, Arumugam VR. Phytosynthesized silver nanoparticles as antiquorum sensing and antibiofilm agent against the nosocomial pathogen Serratia marcescens: an in vitro study. J Appl Microbiol 2018;124(6):1425-1440. http://dx.doi.org/10.1111/jam.13728.
56. Srinivasan R, Vigneshwari L, Rajavel T, Durgadevi R, Kannappan A, Balamurugan K, Pandima Devi K, Veera Ravi A. Biogenic synthesis of silver nanoparticles using Piper betle aqueous extract and evaluation of its anti-quorum sensing and antibiofilm potential against uropathogens with cytotoxic effects: an in vitro and in vivo approach. Environ Sci Pollut Res Int 2018;25(11):10538-10554. http://dx.doi.org/10.1007/s11356-017-1049-0.
57. Qais FA, Shafiq A, Ahmad I, Husain FM, Khan RA, Hassan I. Green synthesis of silver nanoparticles using Carum copticum: Assessment of its quorum sensing and biofilm inhibitory potential against gram negative bacterial pathogens. Microb Pathog 2020; 144:104172. http://dx.doi.org/10.1016/j.micpath.2020.104172.
58. Ali SG, Ansari MA, Sajid Jamal QM, Khan HM, Jalal M, Ahmad H, Mahdi AA. Antiquorum sensing activity of silver nanoparticles in *P. aeruginosa*: an in-silico study. In Silico Pharmacol 2017; 5:12. http://dx.doi.org/10.1007/s40203-017-0031-3.
59. Kanak KR, Dass RS, Pan A. Anti-quorum sensing potential of selenium nanoparticles against LasI/R, RhlI/R, and PQS/MvfR in Pseudomonas aeruginosa: a molecular docking approach. Front Mol Biosci 2023; 10:1203672. http://dx.doi.org/10.3389/fmolb.2023.1203672.
60. Sadoq B, Britel MR, Bouajaj A, et al. In silico study of antiquorum sensing activity of silver, zinc oxide, and copper oxide nanoparticles against Pseudomonas aeruginosa. Research Square 2023. http://dx.doi.org/10.21203/rs.3.rs-2453123/v1.